

Finite- U impurity Anderson model in the presence of an external magnetic field

Kicheon Kang and B. I. Min

Department of Physics, Pohang University of Science and Technology, Pohang 790-784, Korea

(Received 27 November 1995)

We have investigated effects of an external magnetic field in the impurity Anderson model with a finite on-site Coulomb repulsion U . The large- N_f expansion is employed in the slave boson representation, by taking into account f^0 , f^1 , and f^2 subspaces. To evaluate the vertex function for the ‘‘empty state boson’’ self-energy, we have devised two approximations that greatly reduce computational efforts without losing general features of the model. It is found that the Kondo temperature is reduced by the presence of a magnetic field and that at low field and low temperature, the field dependence of both the Kondo temperature and the impurity magnetization exhibits a scaling behavior with high accuracy. Further, several interesting features are found in the field dependence of the impurity magnetization at finite temperature, the physical implications of which are discussed in terms of the renormalized Kondo temperature. [S0163-1829(96)07827-7]

I. INTRODUCTION

Heavy fermion and valence fluctuation phenomena (see, e.g., Refs. 1 and 2) observed in Ce and Yb compounds have often been described by the impurity Anderson model.³ Due to a large on-site Coulomb repulsion U between f electrons, these compounds are considered as typical examples of strongly correlated systems to which the conventional canonical perturbation technique cannot be applied. A systematic large- N_f (N_f is the spin and orbital degeneracy) expansion method has been used for the assumed infinite- U model to describe dynamical as well as thermodynamic properties.^{4,5} The infinite- U treatment allows one to consider only f^0 and f^1 subspaces of f electrons and thus makes the problem quite simple. However, this scheme cannot be justified for realistic systems because U is not infinite (5–6 eV typically). Especially in Ce compounds, f^2 configurations are even energetically comparable to the f^0 configuration.

In the ‘‘spin fluctuation’’ limit (or Kondo limit), the finite- U effect is manifested in various physical properties through the renormalized Kondo temperature T_A . The renormalization of T_A arises from the change of the exchange coupling constant J between conduction electron and f -electron spins due to a finite U , in the sense of the Schrieffer-Wolff transformation.⁶ While this effect was recognized in the exact Bethe ansatz approach⁷ and also in the numerical renormalization-group approach⁸ for $N_f=2$, more appropriate descriptions of the systems with $N_f>2$ were provided by the large- N_f treatments including the f^2 subspace in the variational approach^{1,9} and in the perturbational approach.^{10–15} Using the generalized slave boson technique, Schiller and Zevin¹⁴ have shown that the lowest-order perturbation expansion reproduces the exact $N_f \rightarrow \infty$ variational result at zero temperature ($T=0$).⁹

In this paper, we have investigated effects of an external magnetic field (H) in the finite- U impurity Anderson model, employing the slave boson technique,¹⁶ which is generalized to the finite- U case.¹¹ To our knowledge, there has been no previous study considering both the finite- U and the mag-

netic field effect simultaneously. We obtain the Kondo temperature and the impurity magnetization as a function of U and H . The impurity magnetization at a finite temperature is also determined. In the finite- U case, a set of coupled integral equations appears even in the lowest-order $1/N_f$ expansion. In order to solve the coupled integral equations, we have exploited simplifying approximations, which reduce substantial computational efforts. This treatment allows one to study easily even anisotropic systems, such as those with an external magnetic field or with crystalline fields.

The paper is organized as follows. In Sec. II the large- N_f slave boson theory is formulated for the finite- U impurity Anderson model. In Sec. III approximation schemes used in evaluating the integral equations are described and the U dependence of the Kondo temperature is provided. Section IV is devoted to studying the model in the presence of the external magnetic field both at $T=0$ and at a finite temperature. Special attention is paid to the field dependence of the magnetization. Finally, conclusions are summarized in Sec. V.

II. LARGE- N_f SLAVE BOSON TREATMENT

We consider the finite- U impurity Anderson Hamiltonian in a partial-wave representation

$$\mathcal{H} = \sum_{k,m} \varepsilon_k c_{km}^\dagger c_{km} + \sum_m \varepsilon_{f_m} f_m^\dagger f_m + \sum_{k,m} V(k) (c_{km}^\dagger f_m + f_m^\dagger c_{km}) + U \sum_{m'>m} n_{m'} n_m, \quad (1)$$

where the indices $m, m' (= 1, 2, \dots, N_f)$ denote spin and orbital quantum numbers. The operator c_{km}^\dagger (c_{km}) creates (annihilates) a conduction electron in the state (k, m) with an energy dispersion of $\varepsilon_{\mathbf{k}} = \varepsilon_k$, $k \equiv |\mathbf{k}|$. The f electrons of the magnetic impurity have m -dependent energy ε_{f_m} . The corresponding creation (annihilation) operator and the number operator are f_m^\dagger (f_m) and $n_m = f_m^\dagger f_m$, respectively. The matrix element $V(k)$ represents the hopping of an electron between

the conduction band and the impurity level. We assume that the hopping takes place only between the states with the same m and that the $V(k)$ is independent of m . The Hamiltonian of Eq. (1) is studied in the subspace of at most double occupancy, that is, in the subspace of f^0, f^1 , and f^2 states. This is a good starting point since U is large enough to rule out configurations with more than double occupancies.

Coleman¹⁶ has introduced a single slave boson b to treat the infinite- U model. Then standard many-body techniques can be utilized in this approach without losing the strongly correlated properties of the model. Coleman's method can be generalized to study the finite- U model by introducing a set of "heavy bosons," $d_{mm'}^\dagger = -d_{m'm}^\dagger$.^{11,14,15} The heavy bosons represent $N_f(N_f-1)/2$ doubly occupied f^2 states, energies of which are $E_{2mm'} = \varepsilon_{f_m} + \varepsilon_{f_{m'}} + U$. In this scheme, the Hamiltonian becomes

$$\begin{aligned} \mathcal{H} = & \sum_{k,m} \varepsilon_k c_{km}^\dagger c_{km} + \sum_m \varepsilon_{f_m} f_m^\dagger f_m + \sum_{m>m'} E_{2mm'} d_{mm'}^\dagger d_{mm'} \\ & + \sum_{k,m} V(k) (c_{km}^\dagger b^\dagger f_m + \text{H.c.}) \\ & + \sum_{k,m \neq m'} V(k) (c_{km}^\dagger f_m^\dagger d_{mm'} + \text{H.c.}) \end{aligned} \quad (2)$$

This Hamiltonian commutes with the "charge" operator Q defined by

$$Q \equiv b^\dagger b + \sum_m f_m^\dagger f_m + \sum_{m>m'} d_{mm'}^\dagger d_{mm'}. \quad (3)$$

Physical quantities of the impurity Anderson model should be obtained with the constraint $Q=1$. One way to impose the constraint is to add a "chemical potential" term λQ to \mathcal{H} and to project it onto the physical subspace $Q=1$ by taking $\lambda \rightarrow \infty$ at the end of calculation.¹⁶

With this prescription, the partition function and other quantities are expressed in terms of the spectral functions $\rho_\alpha(\omega)$, $\alpha = b, f_m, d_{mm'}$ corresponding to the f^0, f^1, f^2 states, respectively. The total partition function can be decoupled to a product $Z_c Z_f$, where Z_c is the partition function of the noninteracting conduction electrons and Z_f is the impurity contribution given by

$$Z_f = \int_{-\infty}^{\infty} d\omega e^{-\beta\omega} \left(\rho_b(\omega) + \sum_m \rho_{f_m}(\omega) + \sum_{m>m'} \rho_{d_{mm'}}(\omega) \right). \quad (4)$$

Each of the spectral functions is related to the imaginary part of the corresponding retarded Green's function $G_\alpha(\omega)$:

$$\rho_\alpha(\omega) = -\frac{1}{\pi} \text{Im} G_\alpha(\omega). \quad (5)$$

The Green's functions are written in terms of their self-energies $\Pi, \Sigma_{f_m}, D_{mm'}$:

$$G_b(\omega) = [\omega - \Pi(\omega) + i\delta]^{-1}, \quad (6a)$$

$$G_{f_m}(\omega) = [\omega - \varepsilon_{f_m} - \Sigma_{f_m}(\omega) + i\delta]^{-1}, \quad (6b)$$

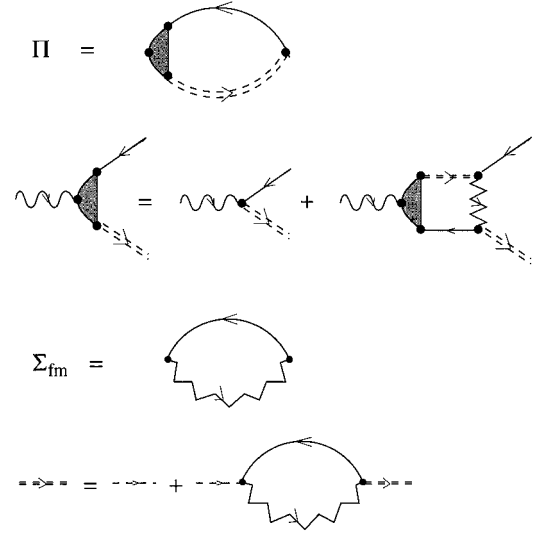


FIG. 1. Lowest-order $[(1/N_f)^0]$ diagrams of the empty boson and the pseudofermion self-energies in the finite- U Anderson model. The full, wiggly, dashed, and jagged lines stand for conduction electron, empty state boson, pseudofermion, and heavy boson propagators, respectively. The double dashed line denotes the renormalized pseudofermion propagator as represented by the diagram in the bottom.

$$G_{d_{mm'}}(\omega) = [\omega - E_{2mm'} - D_{mm'}(\omega) + i\delta]^{-1}, \quad (6c)$$

with a positive infinitesimal number δ . The self-energies can be evaluated by using the noncrossing approximation (NCA), which is generalized for finite U .¹⁰⁻¹⁴ Recall that the NCA has been very successful for the infinite- U model.^{5,16,17} The "generalized NCA" scheme leads to coupled integral equations containing complicated vertex corrections. For this reason, it is practically impossible to solve the equations exactly and so some simplifying approximations are necessary to resolve the problem.

Instead of using the generalized NCA, we adopt here a simple picture of considering only the lowest-order diagrams in $1/N_f$, that is, $(1/N_f)^0$. In fact, crucial finite- U effects are incorporated already in the lowest-order diagrams, as shown below. Figure 1 shows the lowest-order diagrams for the self-energies of the empty boson and the pseudofermion f . The self-energy of the heavy d boson has no contribution in the lowest order. Diagrams in Fig. 1 are calculated by using the standard Feynman rules with the projection procedure mentioned above:

$$\Pi(\omega) = \frac{\Delta}{\pi} \sum_m \int_{-B}^B d\varepsilon f(\varepsilon) G_{f_m}(\omega + \varepsilon) \Gamma_m(\omega; \varepsilon), \quad (7a)$$

with the vertex function

$$\begin{aligned} \Gamma_m(\omega; \varepsilon) = & 1 + \frac{\Delta}{\pi} \sum_{m'(\neq m)} \int_{-B}^B d\varepsilon' f(\varepsilon') G_{f_{m'}}(\omega + \varepsilon') \\ & \times G_{d_{mm'}}(\omega + \varepsilon + \varepsilon') \Gamma_{m'}(\omega; \varepsilon') \end{aligned} \quad (7b)$$

and

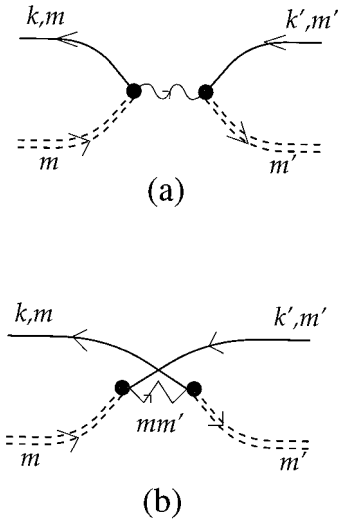


FIG. 2. Two elementary ‘‘spin-flip’’ scattering processes appearing in the empty boson self-energy Π , having (a) an f^0 -intermediate state and (b) an f^2 -intermediate state.

$$\Sigma_{f_m}(\omega) = \frac{\Delta}{\pi} \sum_{m'(\neq m)} \int_{-B}^B d\varepsilon' f(\varepsilon) G_{d_{mm'}}(\omega + \varepsilon), \quad (7c)$$

$$D_{mm'}(\omega) = 0. \quad (7d)$$

Here $f(\varepsilon)$ is the Fermi-Dirac distribution function and $\Delta \equiv \pi \rho(\varepsilon) V^2(\varepsilon)$ is the hopping rate of an electron between the conduction band and the impurity state in a magnetic channel. Here $\rho(\varepsilon)$ is the density of states of the conduction band. The hopping rate is assumed to be a constant Δ for $-B < \varepsilon < B$ and 0 otherwise. Equations (7a)–(7d) with Eq. (6) complete the theory of the lowest order in $1/N_f$. The present treatment reproduces at $T=0$ the exact $N_f \rightarrow \infty$ results of the variational approach.^{9,14}

In the spin fluctuation limit, where f^0 and f^2 configurations are energetically unfavorable relative to f^1 , most important properties of the Anderson model are determined by the b -boson self-energy Π . The Π contains diagrams representing successive ‘‘spin-flip’’ scatterings, which consist of two kinds of processes as shown in Fig. 2. These are the processes that give rise to the coupling constant $J \sim |V|^2/\varepsilon_f - |V|^2/(\varepsilon_f + U)$ between the conduction electron spin and the impurity spin in the Schrieffer-Wolff transformation.¹² While process (a) in Fig. 2 is present in the infinite- U model having an f^0 intermediate state, process (b), which contains the d -boson line as an intermediate state, does not exist in the infinite- U model. Process (b), which comes out from the vertex function Γ_m in the empty boson self-energy, leads to a renormalization of the Kondo temperature T_A through the modification of the coupling constant $J(U)$ and $T_A(U) \sim B \exp[1/N_f J(U) \rho(0)]$.

III. APPROXIMATIONS AND THE KONDO TEMPERATURE

Thermodynamic properties of the finite- U impurity Anderson model in the restricted subspaces f^0 , f^1 , and f^2 are determined entirely by the spectral functions $\rho_\alpha(\omega)$. The ground-state energy E_0 is obtained from the lowest pole of

$\rho_b(\omega)$ at $T=0$, which corresponds to a nonmagnetic ground state. Using Eq. (7a), one gets the following equation for E_0 :

$$E_0 = \Pi(E_0), \quad (8)$$

with Π calculated at $T=0$, where E_0 is real. Similarly, the lowest poles of $\rho_{f_m}(\omega)$ yield magnetic excited energies $\tilde{\varepsilon}_{f_m}$ satisfying

$$\tilde{\varepsilon}_{f_m} - \varepsilon_{f_m} - \Sigma_{f_m}(\tilde{\varepsilon}_{f_m}) = 0. \quad (9)$$

$\Sigma_{f_m}(\tilde{\varepsilon}_{f_m})$ has no imaginary part in the temperature range of interest $T \lesssim T_A$. The ‘‘Kondo temperature’’ T_A , which is defined by the difference between the ground-state energy E_0 and the lowest excited-state energy $\min\{\tilde{\varepsilon}_{f_m}\}$, characterizes the low-temperature and low-energy properties of the model. E_0 and $\tilde{\varepsilon}_{f_m}$ calculated in this fashion reproduce the exact $N_f \rightarrow \infty$ ground state and the excited-state energy, respectively, obtained by the variational approach.^{9,14}

To get E_0 , one should solve numerically the set of coupled integral equations involving the vertex function Γ_m . Note that in the infinite- U case, $\Gamma_m = 1$. To solve the equation, we have devised two simple approximations, which can be readily applied to anisotropic systems without much computational efforts. In Γ_m , there are two independent energy variables ω and ε . While Γ_m has a large dependence on ω near $\omega = E_0$ due to $G_{f_m}(\omega + \varepsilon')$ in the integrand of the Eq. (7b), it has relatively a weak dependence on ε . It is because the ε dependence of Γ_m exists only in $G_{d_{mm'}}(\omega + \varepsilon + \varepsilon') = (\omega + \varepsilon + \varepsilon' - E_{2mm'})^{-1}$ and this dependence would be negligible for large U . Thus we replace $\Gamma_{m'}(\omega; \varepsilon')$ in the integrand by $\Gamma_{m'}(\omega; \varepsilon)$ to avoid solving the coupled integral equations. Actually, this corresponds to neglecting some energy conservation in the vertex function diagram of Fig. 1. However, owing to the weak dependence on ε of Eq. (7b), this approximation turns out to be quite good, as will be shown below. The resulting equation reads

$$\Gamma_m(\omega; \varepsilon) = 1 + \frac{\Delta}{\pi} \sum_{m'(\neq m)} \Lambda_{mm'}(\omega; \varepsilon) \Gamma_{m'}(\omega; \varepsilon), \quad (10a)$$

where

$$\Lambda_{mm'}(\omega; \varepsilon) = \int_{-B}^B d\varepsilon' f(\varepsilon') G_{f_m}(\omega + \varepsilon') G_{d_{mm'}}(\omega + \varepsilon + \varepsilon'). \quad (10b)$$

Now Eq. (10a) is merely a linear algebraic equation of Γ_m 's for given energy variables ω, ε . This is our first approximation (I).

The equation can be further simplified by representing the pseudofermion Green's function as

$$G_{f_m}(\omega) = \frac{z_{f_m}}{\omega - \tilde{\varepsilon}_{f_m} + i\delta}, \quad (11a)$$

where z_{f_m} is the renormalization coefficient at $\omega = \tilde{\varepsilon}_{f_m}$ defined by

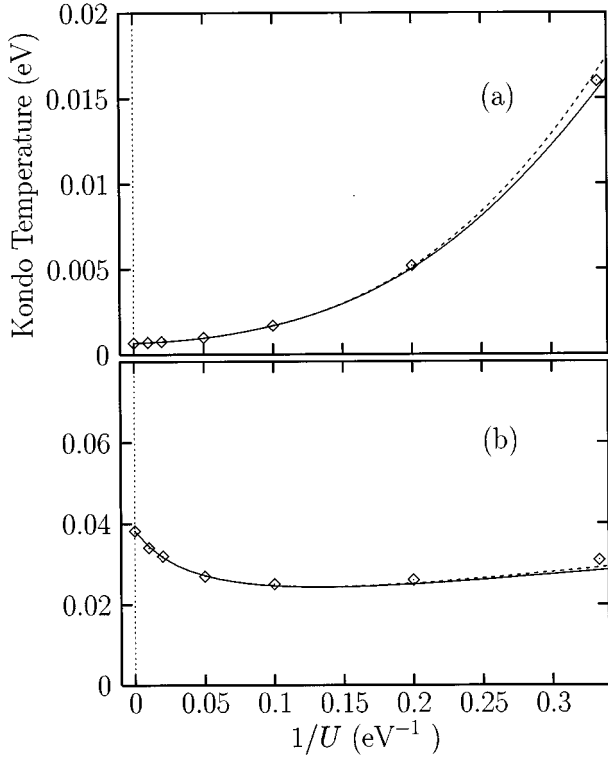


FIG. 3. Comparison of the present results for the Kondo temperature with the exact $N_f \rightarrow \infty$ variational results at $T=0$ (Ref. 9). Dashed (solid) lines are the Kondo temperatures obtained by the approximation scheme I (I and II) and points correspond to the exact variational temperatures. Parameters used here are $N_f = \infty$, $\tilde{\Delta} = N_f \Delta = 0.75$ eV, and $B = 24$ eV with (a) $\varepsilon_f = -2.5$ eV and (b) $\varepsilon_f = -1.5$ eV. Here the degenerate f level $\varepsilon_{f_m} = \varepsilon_f$ is assumed.

$$z_{f_m} = \left(1 - \frac{\partial}{\partial \omega} \text{Re} \Sigma_{f_m}(\omega) \right)^{-1} \Big|_{\omega = \tilde{\varepsilon}_{f_m}}. \quad (11b)$$

This representation is quite reasonable for large U since the incoherent background of G_{f_m} is located at very high energy ($\omega > E_{2mm'}$) as compared to $\tilde{\varepsilon}_{f_m}$ and the weight of the incoherent part ($1 - z_{f_m}$) would be very small (note that it becomes zero for infinite U). Thus, replacing G_{f_m} by Eq. (11a) makes no practical difference in evaluating Eq. (10b) and the effect is minimal for large U . Then $\Lambda_{mm'}$ in Eq. (10b) can be obtained analytically at $T=0$,

$$\Lambda_{mm'}(\omega; \varepsilon) = \frac{z_{f_m'}}{E_{2mm'} - \tilde{\varepsilon}_{f_m} - \varepsilon} \times \ln \left(\frac{\tilde{\varepsilon}_{f_m} - \omega + B}{\tilde{\varepsilon}_{f_m} - \omega} \frac{E_{2mm'} - \omega - \varepsilon}{E_{2mm'} - \omega - \varepsilon + B} \right). \quad (12)$$

This is our second approximation (II).

The present approximation schemes yield fairly good results of the ground-state energy E_0 and the Kondo temperature T_A for $U \geq 5$ eV. As shown in Fig. 3, in the large- U limit ($U \gg B$), the Kondo temperature as a function of $1/U$

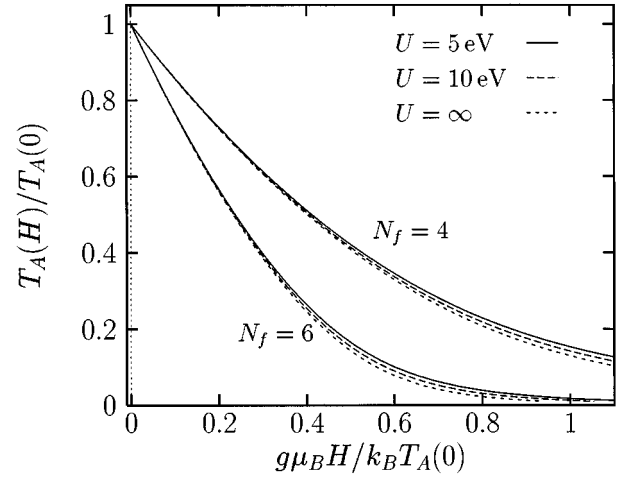


FIG. 4. Normalized Kondo temperature vs normalized magnetic field strength for $N_f=4$ and $N_f=6$. The normalized Kondo temperatures are almost the same for different U 's. Other parameters used are $\varepsilon_f = -2$ eV, $\tilde{\Delta} = 0.9$ eV, and $B = 3$ eV.

increases or decreases depending on the parameters ε_f , $\tilde{\Delta} = N_f \Delta$, and B .⁹ Results obtained by using both approximations I and II are close to those obtained by using approximation I only. Furthermore, both results are in good agreement with those of the exact $N_f \rightarrow \infty$ variational approach. This demonstration indicates that the approximations (I and II) we employed are very reasonable at least for large U . Deviations from the results of the variational calculation are apparent for smaller U because the present approximation schemes become less accurate for small U , as mentioned above. We used in Fig. 3 quite a large value of the half bandwidth $B = 24$ eV. One can conjecture that approximation I works better for a realistic smaller bandwidth, e.g., $2B < O(10$ eV), because, for smaller B , the ε' dependence of the vertex function $\Gamma_{m'}(\omega, \varepsilon')$ in the integrand of Eq. (7b) would be weaker.

IV. SCALINGS IN THE PRESENCE OF THE EXTERNAL MAGNETIC FIELD

With the approximation schemes described in the preceding section, we investigate effects of the external magnetic field in the finite- U impurity Anderson model. By applying the external field $\vec{H} = H \hat{z}$ to a degenerate system ($\varepsilon_{f_m} = \varepsilon_f$), Zeeman splitting occurs in the localized f levels: $\varepsilon_{f_m} = \varepsilon_f + g \mu_B H m$, $m = -j, -j+1, \dots, j$ ($2j+1 = N_f$). Conduction electron polarization is neglected since its contribution is perturbatively small.¹⁸

The Kondo temperature in the presence of H is also obtained from the energy difference between the ground state and the lowest excited-state energy. Figure 4 plots the magnetic field dependence of T_A . T_A 's are normalized by their zero-field values as given in Table I. It is seen that T_A decreases with increasing H . A reduction of the Kondo temperature by the applied field originates from the reduction of the ground-state binding energy. The applied field lifts up the degeneracy of the f level to decrease the effective degeneracy. Hence the binding energy will be reduced exponen-

TABLE I. Kondo temperature T_A at $H=0$ for $N_f=4$ and $N_f=6$. Parameter sets are the same as those in Fig. 4.

U (eV)	T_A (meV) ($N_f=4$)	T_A (meV) ($N_f=6$)
∞	2.76	2.76
10	6.04	6.51
5	11.9	13.4

tially, recalling that $T_A \sim B \exp \pi \epsilon_f / N_f \Delta$ in the Kondo limit of the infinite- U model. Notable in this figure is that $T_A(H)/T_A(0)$ exhibits almost the same functional form against $g \mu_B H / k_B T_A(0)$ regardless of the size of U , implying that the scaling behavior holds with high accuracy in the low-field region. In contrast, $T_A(H)/T_A(0)$ has a different scaling behavior for different N_f . In the infinite- U limit, $T_A(H)/T_A(0)$ can be expressed as (see the Appendix)

$$\frac{T_A(H)}{T_A(0)} = \frac{1}{\prod_{m=1}^{N_f-1} \left[\left(1 + m \frac{g \mu_B H / T_A(0)}{T_A(H)/T_A(0)} \right)^{1/N_f} \right]} \times \exp \left[\frac{\pi}{\Delta} (E_0(H) - E_0(0)) \right]. \quad (13)$$

The solution of Eq. (13) can be regarded as an N_f -dependent scaling function characterizing the low- T and low- H properties of the model. Using the Kondo temperature T_A rescaled by U , the scaling of Eq. (13) will be also valid in the finite- U case.

The impurity contribution to the magnetization M^{imp} of the system can be obtained from the relation

$$M^{\text{imp}} = \frac{1}{\beta} \frac{\partial}{\partial H} \ln Z_f. \quad (14)$$

The ground state is no longer nonmagnetic in the presence of the magnetic field, since the field polarizes both the impurity electrons and the conduction electrons. In Fig. 5 the ground-state impurity magnetization $M^{\text{imp}}(H)$ is plotted as a function of $g \mu_B H / k_B T_A(0)$. The magnetization in this figure is normalized by its saturation value $M_{\text{sat}}^{\text{imp}} = j g \mu_B$. The magnetization at low field also shows a scaling behavior almost perfectly, as in the case of $T_A(H)$. The present results of $M^{\text{imp}}(H)$ are compared with the Bethe ansatz results for the Coqblin-Schrieffer model.¹⁹ In the Bethe ansatz results appears the low-temperature scale T_L , which is related to the zero-temperature susceptibility $\chi_0 = (g \mu_B)^2 j(j+1) / 3 T_L$. On the other hand, the susceptibility in our treatment is given by $\chi_0 = n_f (g \mu_B)^2 j(j+1) / 3 T_A$ for $U = \infty$. By considering the relationship between two energy scales, it is possible to compare our results with the Bethe ansatz results. As is seen in Fig. 5, the present results of $M^{\text{imp}}(H)$ agree quite well with the Bethe ansatz results in the low-field region, even though they are a bit overestimated in the high-field region. The deviation from the exact results at high-field indicates that the $1/N_f$ expansion may not work well in the high-field region. As mentioned previously, the applied field splits the f level and reduces the effective degeneracy and so the lowest-order $1/N_f$ expansion becomes invalid in the high-

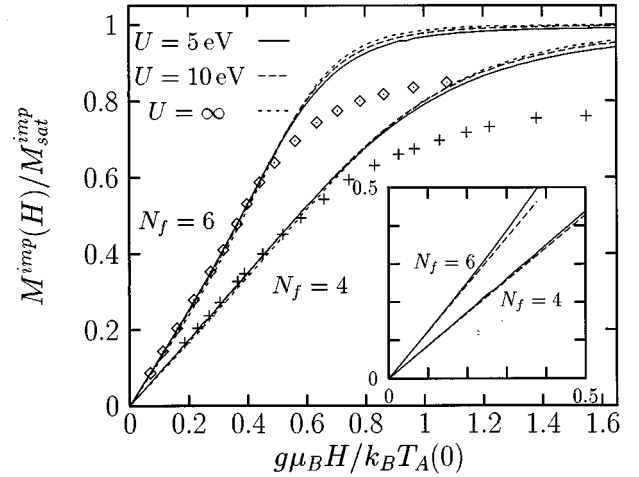


FIG. 5. Scaling behavior of the impurity magnetization that is normalized by its saturation value $M_{\text{sat}}^{\text{imp}} = j g \mu_B$. Bethe ansatz results of the Coqblin-Schrieffer model for $N_f=4$ (+) and $N_f=6$ (\diamond) are also given for comparison. The inset shows deviations of the low-field magnetizations from linearity for $N_f=4$ and $N_f=6$. Solid lines are the present results for $U=5$ eV and dashed lines are extrapolated values from the initial slope $\partial m / \partial h|_{h=0} h$. Other parameters are the same as those in Fig. 4.

field region. It is noteworthy that the overestimation of $M^{\text{imp}}(H)$ observed in Fig. 5 is also found in the infinite- U NCA scheme for large H/T .²⁰

An interesting feature is found in the low-field magnetization. The inset of Fig. 5 indicates that the low-field magnetization increases more rapidly than linearly in H . This deviation from the linearity, the so-called superlinear behavior, has been reported by Hewson *et al.*,¹⁹ based on the Bethe ansatz solution of the Coqblin-Schrieffer model. They found that the superlinearity occurs for $N_f > 3$ and that the experimental results of YbCuAl are well described by their $N_f=8$ model. The superlinearity is also revealed by the finite-temperature NCA scheme²⁰ as well as by the mean-field approximation²¹ in the infinite- U , large- N_f treatments of the Anderson model. The superlinear behavior has its origin in the fact that the Kondo resonance, which is located near T_A above the Fermi level, becomes narrower as N_f increases. That is, the Kondo resonance is sharply defined for large N_f , implying a strong screening effect. As a consequence, the spin polarization does not begin to dominate until the magnetic field becomes comparable to T_A . As the Zeeman energy is comparable to $k_B T_A$, the magnetic field overcomes the screening by conduction electrons and the spin polarization dominates the system. It is quite natural that the superlinearity is present in our finite- U model, in view of the almost perfect scaling of $M^{\text{imp}}(H)$ in the low-field regime. The superlinearity persists at low T/T_A , but disappears at higher temperature because of suppression of the Kondo resonance.

At finite temperature, the situation is more intriguing. For a given low T , $M^{\text{imp}}(H)$ shows an upturn at a certain field H^* (denoted by arrows in Fig. 6), apart from the superlinearity at lower field. Making a further investigation into this anomaly, one could find that the Kondo temperature at the upturn point is nearly equal to a given temperature of the

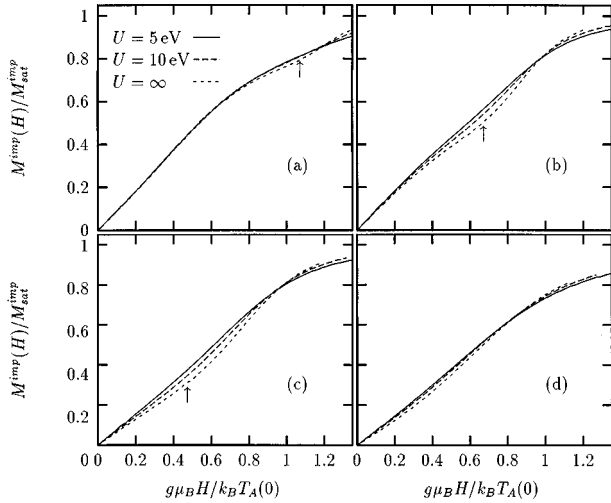


FIG. 6. Field dependence of the magnetization for $N_f=4$ at (a) $T/T_A=0.1$, (b) $T/T_A=0.3$, (c) $T/T_A=0.5$, and (d) $T/T_A=0.9$. Other parameters are the same as those in Fig. 4. Arrows in (a)–(c) denote upturns of the magnetization. The upturn smears out at higher temperature as shown in (d).

system, that is, $T_A(H^*) \approx T$. This phenomenon could be understood as follows. For a given low T , $M^{\text{imp}}(H)$ has a superlinearity at low H , but diminishes its increasing rate for intermediate values of H . As H increases further, $M^{\text{imp}}(H)$ exhibits an upturn at $H=H^*$ that fulfills $T_A(H^*) \approx T$. It takes place because the population in the lowest excited magnetic state increases abruptly at the point satisfying $T_A(H^*) \approx T$, producing observed upturns at H^* . It is shown in Fig. 6 that the upturn smears out at higher temperature since the Kondo resonance is suppressed at high temperature. Another thing to note is that the scaling of $M^{\text{imp}}(H)$ at finite T is not as good as that at $T=0$.

Figure 7 presents $M^{\text{imp}}(H)$ for $U=5$ eV at various temperatures. Nonmonotonicity as a function of T is apparent in

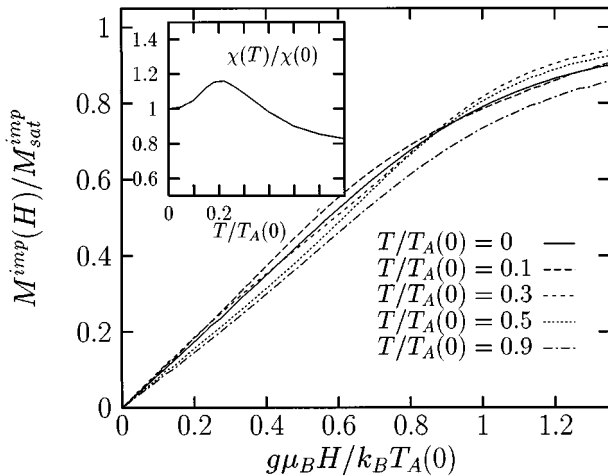


FIG. 7. Field dependence of the magnetization for various temperatures with $N_f=4$ and $U=5$ eV. Other parameters used are the same as those in Fig. 4. The inset shows the nonmonotonic behavior of the magnetic susceptibility divided by its value of $T=0$, $\chi(T)/\chi(0)$.

the low-field magnetization. With increasing the temperature, $M^{\text{imp}}(H)$ for a given small H , which is proportional to magnetic susceptibility, increases first at low T , but after reaching a maximum at an intermediate T^* , $M^{\text{imp}}(H)$ decreases at higher T (see the inset of Fig. 7). This nonmonotonic behavior in the temperature dependence of the magnetic susceptibility is known to be more pronounced for a system with larger N_f (Ref. 22) and is considered to have the same origin as that of the superlinearity in $M^{\text{imp}}(H)$.²⁰

V. CONCLUSION

We have studied the finite- U impurity Anderson model in the presence of an external magnetic field. The large- N_f expansion considering f^0 , f^1 , and f^2 subspaces in the slave boson representation is employed to take into account finite- U effects. The lowest-order treatment gives rise to a complicated vertex function in the empty boson self-energy and a renormalization of f -level energies. We have devised two simple approximation schemes to evaluate the vertex function. One consists of transforming the integral equation into an algebraic equation by assuming that the vertex function has a weak dependence on one of two energy variables. The other is to simplify the pseudofermion Green's function by neglecting the incoherent part. These approximations reduce computational efforts substantially and are shown to yield fairly good results for $U \geq 5$ eV.

This treatment has been applied to the system with an external magnetic field. It is found that the Kondo temperature is reduced by the magnetic field. Scaling behaviors in the field dependence of the Kondo temperature and the impurity magnetization are found to hold almost perfectly at low field and low temperature. This implies that the main effect of the finite U in the presence of the magnetic field is manifested through the renormalization of the Kondo temperature. Some intriguing features are found in the field dependence of the magnetization, such as superlinearity at low field and upturns at a higher field H^* for a given low temperature, which are expected to occur from a competition between the singlet binding energy and the Zeeman energy gain of electrons.

ACKNOWLEDGMENTS

This work was supported by the POSTECH-BSRI program of the Korean Ministry of Education (Grant No. BSRI-95-2438) and in part by the Korea Science Engineering Foundation through the SRC program of SNU-CTP.

APPENDIX

Let us consider the Kondo temperature in the presence of the applied magnetic field for the $U=\infty$ case. Degenerate f levels split by the magnetic field. The energy levels can be expressed in terms of the Kondo temperature, as defined in Sec. III:

$$\varepsilon_{f_m} = E_0(H) + T_A(H) + m g \mu_B H, \quad (\text{A1})$$

where $m=0,1,2,\dots,N_f-1$. In the $U \rightarrow \infty$ limit, Eq. (8) reduces to

$$E_0(H) = \frac{\Delta}{\pi} \sum_m \int_{-B}^0 \frac{d\varepsilon}{E_0(H) - \varepsilon - \varepsilon_{f_m}} \quad (\text{A2})$$

at $T=0$. An analytical evaluation of Eq. (A2) with Eq. (A1) yields

$$E_0(H) = \frac{\tilde{\Delta}}{\pi} \ln \frac{T_A}{B} \left\{ \prod_{m=0}^{N_f-1} \left(1 + m \frac{g\mu_B H}{T_A(H)} \right) \right\}^{1/N_f}. \quad (\text{A3})$$

In the derivation, we used the condition $B \gg N_f g \mu_B H$ and $B \gg T_A$. Equation (A3) corresponds to Eq. (13).

-
- ¹See, e.g., O. Gunnarsson and K. Schönhammer, in *Handbook on the Physics and Chemistry of Rare Earths*, edited by K. A. Gschneidner, Jr., L. Eyring, and S. Hufner (North-Holland, Amsterdam, 1987), Vol. 10, pp. 103–163, and references therein.
- ²N. Grewe and F. Steglich, in *Handbook on the Physics and Chemistry of Rare Earths* (Ref. 1), pp. 343–474, and references therein.
- ³P. W. Anderson, Phys. Rev. **124**, 41 (1961).
- ⁴O. Gunnarsson and K. Schönhammer, Phys. Rev. B **28**, 4315 (1983).
- ⁵N. E. Bickers, Rev. Mod. Phys. **59**, 845 (1987), and references therein.
- ⁶J. R. Schrieffer and P. A. Wolff, Phys. Rev. **149**, 491 (1966); B. Coqblin and J. R. Schrieffer, *ibid.* **185**, 847 (1969).
- ⁷A. M. Tselick and P. B. Wiegman, Adv. Phys. **32**, 453 (1983).
- ⁸H. R. Krishna-murthy, J. W. Wilkins, and K. G. Wilson, Phys. Rev. B **21**, 1003 (1980); **21**, 1044 (1980).
- ⁹O. Gunnarsson and K. Schönhammer, Phys. Rev. B **31**, 4815 (1985).
- ¹⁰O. Sakai, M. Motizuki, and T. Kasuya, in *Core-Level Spectroscopy in Condensed Systems*, edited by J. Kanamori and A. Kotani, Springer Series in Solid-State Sciences Vol. 81 (Springer, Berlin, 1988), p. 45.
- ¹¹J. Holm and K. Schönhammer, Solid State Commun. **69**, 969 (1989).
- ¹²Th. Pruschke and N. Grewe, Z. Phys. B **74**, 439 (1989).
- ¹³H. Keiter and Q. Qin, Physica B **163**, 594 (1990); Q. Qin and H. Keiter, Z. Phys. B **84**, 89 (1991).
- ¹⁴A. Schiller and V. Zevin, Phys. Rev. B **47**, 9297 (1993).
- ¹⁵J. Holm, R. Kree, and K. Schönhammer, Phys. Rev. B **48**, 5077 (1993).
- ¹⁶P. Coleman, Phys. Rev. B **29**, 3035 (1984).
- ¹⁷Y. Kuramoto, Z. Phys. B **53**, 37 (1983).
- ¹⁸J. H. Lowenstein, Phys. Rev. B **29**, 4120 (1984).
- ¹⁹A. C. Hewson, J. W. Rasul, and D. M. Newns, Phys. Lett. **93A**, 311 (1983); A. C. Hewson and J. W. Rasul, J. Phys. C **16**, 6799 (1983); A. C. Hewson, J. W. Rasul, and D. M. Newns, Solid State Commun. **47**, 59 (1983).
- ²⁰D. L. Cox, Phys. Rev. B **35**, 4561 (1987).
- ²¹D. M. Newns, N. Read, and A. C. Hewson, in *Moment Formation in Solids*, edited by W. J. M. Buyers (Plenum, New York, 1984), p. 257; D. M. Newns and N. Read, Adv. Phys. **36**, 799 (1987).
- ²²V. T. Rajan, Phys. Rev. Lett. **51**, 308 (1983).